

# HIGH-FREQUENCY InGaAs/InP MULTIPLE-QUANTUM-WELL BURIED-MESA ELECTROABSORPTION OPTICAL MODULATOR

Indexing terms: Optical modulation, Semiconductor devices and materials

We describe the structure and performance characteristics of an InGaAs/InP multiple-quantum-well (MQW) electro-absorption buried-mesa optical modulator. The device is fabricated with two metal-organic chemical-vapour-deposition (MOCVD) growth steps, wherein small-area circular (40  $\mu\text{m}$  diameter) PIN diodes are buried with Fe-doped semi-insulating (SI) InP regrowth. The modulator has a relatively low insertion loss (4.5 dB) with 25% modulation depth and very high modulation bandwidth (5.3 GHz) operating at 1.62  $\mu\text{m}$  wavelength.

Multiple-quantum-well (MQW) PIN modulators based on the quantum confined Stark effect have been demonstrated in the GaAs/GaAlAs material system. These include both mesa-type PIN modulators<sup>1,2</sup> and waveguide modulators.<sup>3</sup> These modulators make use of the shift in the excitonic absorption edge towards longer wavelengths as an external electric field is applied perpendicular to the plan of the quantum wells.<sup>4</sup> There is, however, a strong motivation to develop MQW modulators in the InGaAsP/InP material system because of the wide wavelength range available and the applications for transmission through low-loss optical fibres.

MQW waveguide electroabsorption modulators have been demonstrated in the InGaAs/InAlAs material system grown by molecular beam epitaxy (MBE).<sup>5,6</sup> Recently, the growth of high-quality InGaAs/InP MQW material by atmospheric-pressure metal-organic chemical vapour deposition (MOCVD) has been reported.<sup>7,8</sup> This material system has been used for the fabrication of several devices such as lasers,<sup>7</sup> low-loss MQW waveguides<sup>9</sup> and MQW waveguide phase modulators.<sup>10</sup> The quantum confined Stark effect has been demonstrated and measured for this material using etched mesa PIN diodes with large dimensions (200  $\times$  200  $\mu\text{m}$ ).<sup>11</sup>

In this letter we report a buried mesa PIN electro-absorption amplitude modulator with low insertion loss and high modulation bandwidth. The high-frequency response was obtained by reducing the size of the PIN mesa to 40  $\mu\text{m}$  diameter, and using a selective regrowth of Fe-doped semi-insulating (SI) InP by MOCVD to bury the side walls of the mesa. The bonding pad for the mesa contact is located on the semi-insulating material. Therefore, the parasitic capacitance is minimal and high-frequency operation can be obtained.

**Modulator structure and fabrication:** A cross-section schematic diagram of the device is shown in Fig. 1. The device is fabricated in two epitaxial growth steps using an atmospheric-pressure MOCVD system as described in Reference 8. The base wafer is grown on a p-InP substrate and consists of a p-InP buffer layer (Zn-doped at  $10^{18} \text{ cm}^{-3}$ ) followed by 100 InGaAs quantum wells of 100  $\text{\AA}$  thickness with 100  $\text{\AA}$  InP

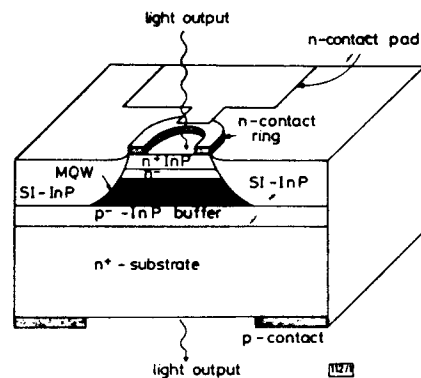


Fig. 1 Schematic diagram of device

barriers (undoped). This is followed by a 0.3  $\mu\text{m}$  n-InP buffer layer (undoped) and a top n-InP contact layer (S-doped at  $2 \times 10^{18} \text{ cm}^{-3}$ ). After the first growth, circular mesas of 40  $\mu\text{m}$  diameter and 5  $\mu\text{m}$  depth are chemically etched using  $\text{SiO}_2$  masks; the mesas are then buried with an Fe-doped semi-insulating InP regrowth using the same  $\text{SiO}_2$  masks for the selective regrowth.

The top n-contact is an alloyed AuGe/Au ring with 20 and 40  $\mu\text{m}$  inner and outer diameters, respectively. This ring is in contact with a Cr/Au pad deposited by a standard lift-off technique. The bonding pad is located on the semi-insulating InP as shown in Fig. 1. The p-contact metallisation on the back side has a 100  $\mu\text{m}$  aperture located under each of the active mesas so that the modulated light beam can be detected on the output side.

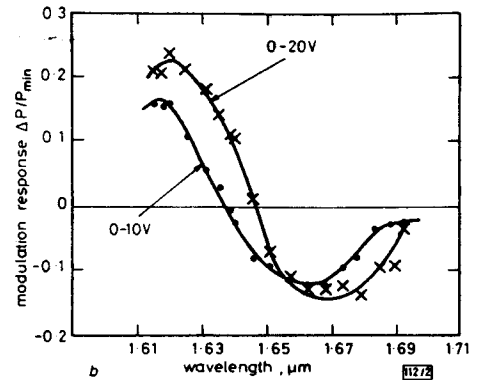
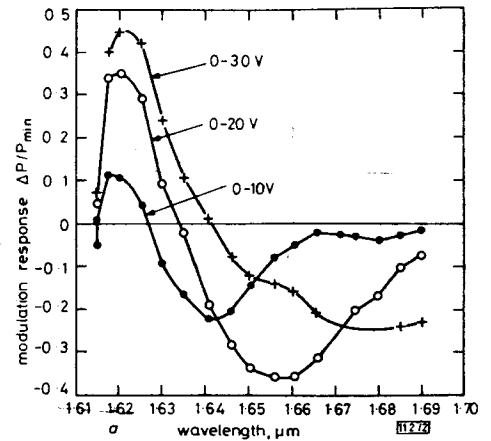


Fig. 2 Modulation response (e.g. the difference between the optical powers with and without applied voltage divided by the smaller of these values) against wavelength for different modulation voltages

a For a buried small-area circular mesa device  
b For a large (200  $\times$  200  $\mu\text{m}$ ) etched mesa

**Results and discussion:** The CW modulation response curves of the buried PIN mesa and of a large-area (200  $\times$  200  $\mu\text{m}$ ) etched mesa without the SI-InP regrowth are shown in Figs. 2a and b, respectively. Typical diodes have reverse-breakdown voltages of 30–40 V and dark currents of less than 1  $\mu\text{A}$ . The modulation characteristics were measured using a tunable external-cavity-grating semiconductor laser. The collimated laser light beam was focused on the modulator and collected at the output using two objective lenses. The total insertion loss was 4.5 dB. Most of this loss is due to reflections at the air/semiconductor interfaces and to the absorption in the p-substrate.

It is interesting to note that, depending on the relative position of the laser wavelength and the quantum-well bandgap, it is possible to obtain either increased or reduced transmission with increased electric field. The maximum modulation depth is obtained at about 1.62  $\mu\text{m}$ , which corresponds to the peak

of the exciton absorption with no field applied. At this wavelength the modulation is positive since the transmitted light is increased with electric field because of the shift of the excitonic resonance to a longer wavelength.<sup>11</sup> At longer wavelengths the modulation response has an opposite sign with maximum negative modulation response at about 1.675  $\mu\text{m}$ . In this region of the spectrum the broadening of the exciton peak also contributes to the modulation response.<sup>11</sup>

The maximum modulation depth for the buried-mesa device is 25% (Fig. 2a). This is significantly smaller than the 45% modulation depth obtained for a large-area etched mesa (Fig. 2b). This indicates some degradation in performance following the regrowth process, which might be due to thermal diffusion of dopants (especially zinc) during the regrowth.

For high-frequency measurements, the semi-insulating buried PIN diode was mounted on a copper stud fitting into a high-frequency microwave test fixture. The output from the modulator was detected using a 36 GHz-bandwidth InGaAs PIN photodiode.<sup>12</sup> The overall modulation response was measured using a microwave network analyser (HP 8510). The small-signal high-frequency modulation response at different bias voltages is shown in Fig. 3. The high-frequency roll-off is independent of bias voltage. There is a bias-dependent roll-off at frequencies up to 1 GHz, but the response is reasonably flat out to nearly 5 GHz for bias voltages around 7 V. The 3 dB small-signal modulation bandwidth for this device was 5.3 GHz at 1.621  $\mu\text{m}$  wavelength. This modulation bandwidth is, to our knowledge, the highest yet reported for an electro-absorption optical modulator.

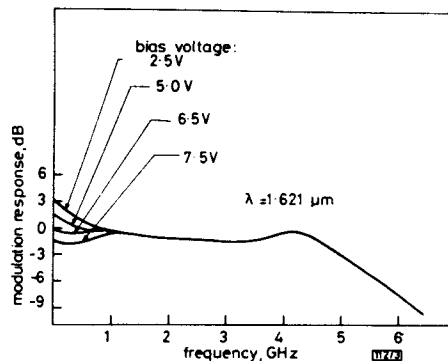


Fig. 3 Small-signal modulation response of buried-mesa device for different bias voltages

**Conclusions:** An electroabsorption optical modulator based on the quantum confined Stark effect in InGaAs/InP MQW material has been described. A very high modulation bandwidth (5.3 GHz) has been obtained with small-area circular (40  $\mu\text{m}$ -diameter) mesa diodes buried with a semi-insulating InP regrowth.

U. KOREN  
B. I. MILLER  
R. S. TUCKER  
G. EISENSTEIN  
I. BAR-JOSEPH  
D. A. B. MILLER  
D. S. CHEMLA

AT&T Bell Laboratories  
Holmdel, NJ 07733, USA

18th March 1987

#### References

- WOOD, T. H., BURRUS, C. A., MILLER, D. A. B., CHEMLA, D. S., DAMEN, T. C., GOSSARD, A. C., and WIEGMANN, W.: 'High speed optical modulation with GaAs/GaAlAs QW in p-i-n diode structure', *Appl. Phys. Lett.*, 1984, 44, pp. 16-18
- WOOD, T. H., BURRUS, C. A., MILLER, D. A. B., CHEMLA, D. S., DAMEN, T. C., GOSSARD, A. C., and WIEGMANN, W.: '131 ps optical modulation in semiconductor MQW', *IEEE J. Quantum Electron.*, 1985, QE-21, pp. 117-118
- WEINER, J. S., MILLER, D. A. B., CHEMLA, D. S., DAMEN, T. C., BURRUS, C. A., WOOD, T. H., GOSSARD, A. C., and WIEGMANN, W.: 'Strong polarization sensitive electroabsorption in GaAs/GaAlAs QW waveguides', *Appl. Phys. Lett.*, 1985, 47, pp. 1148-1150

- MILLER, D. A. B., CHEMLA, D. S., DAMEN, T. C., GOSSARD, A. C., WIEGMANN, W., WOOD, T. H., and BURRUS, C. A.: 'Electric field dependence of optical absorption near the band-gap of QW structures', *Phys. Rev. B*, 1985, 32, pp. 1043-1060
- WAKITA, K., KAWAMURA, Y., YOSHIKUNI, Y., ASAH, H., and UEHARA, S.: 'Anisotropic electroabsorption and optical modulation in InGaAs/InAlAs MQW structures', *IEEE J. Quantum Electron.*, 1986, QE-22, pp. 1831-1836
- KAWAMURA, Y., WAKITA, K., YOSHIKUNI, Y., ITAYA, Y., and ASAH, H.: 'Monolithic integration of DFB lasers and MQW optical modulators'. Technical digest of the 10th int. semiconductor laser conference, Kanazawa, Japan, 1986, Paper B-4, pp. 22-23
- NELSON, A. W., WONG, S., REGNAULT, J. C., HOBBS, R. E., MURREL, D. L., and WALLING, R. H.: 'DH and multi quantum well lasers at 1.5-1.7  $\mu\text{m}$  grown by atmospheric pressure MOVPE', *Electron. Lett.*, 1985, 21, pp. 329-331
- MILLER, B. I., SCHUBERT, E. F., KOREN, U., OURMAZD, A., DAYEM, A. H., and CAPIK, R. J.: 'High quality narrow GaInAs/InP QW grown by atmospheric OMVPE', *Appl. Phys. Lett.*, 1986, 49, pp. 1384-1386
- KOREN, U., MILLER, B. I., KOCH, T. L., BOYD, G. D., CAPIK, R. J., and SOCCOLICH, C. E.: 'Low-loss InGaAs/InP MQW waveguide', *ibid.*, 1986, 49, pp. 1602-1604
- KOREN, U., KOCH, T. L., PRESTING, H., and MILLER, B. I.: 'InGaAs/InP multiple quantum well waveguide phase modulator', *ibid.*, 1987, 50, pp. 368-370
- BAR-JOSEPH, I., KLINGSHIRN, C., MILLER, D. A. B., CHEMLA, D. S., KOREN, U., and MILLER, B. I.: 'Quantum confined Stark effect in InGaAs/InP quantum wells grown by OMVPE'. Technical digest of the picosecond electronics conference, Lake Tahoe, NV, Jan. 1987, pp. 162-164
- BURRUS, C. A., BOWERS, J. E., and TUCKER, R. S.: 'Improved very-high-speed packaged InGaAs PIN punch-through photodiode', *Electron. Lett.*, 1985, 21, pp. 262-263

#### GaAs/GaAlAs RIB WAVEGUIDE GRATING FILTERS FOR $\lambda = 1.5 \mu\text{m}$

**Indexing terms:** Optical communications, Semiconductor devices and materials, Optical filters

First-order Bragg grating filters have been realised in GaAs/GaAlAs rib waveguides for operation at  $\lambda \sim 1.5 \mu\text{m}$ . Single-mode devices with rib widths of 2 to 5  $\mu\text{m}$  and incorporating a 2.5 mm length of 225 nm period grating have been evaluated using a tunable Ti:KCl colour-centre laser. Rejection ratios of 95% to 39% and 3 dB bandwidths of 3.5 Å to 7.9 Å have been measured.

Narrowband optical filters are key components in closely spaced wavelength-multiplexed fibre networks. Guided-wave grating filters have narrowband response and are potential candidates in applications requiring stopband characteristics.

The operation principle of thin-film optical grating filters is well understood.<sup>1,2</sup> A single-mode waveguide with a periodic surface corrugation of period  $\Lambda$  will cause the normally incident mode, with guide wavelength  $\lambda_g$ , to autoreflect if the Bragg condition  $\lambda_g = 2\Lambda$  is satisfied. Light of other wavelengths passes through the grating virtually unaffected. At the Bragg wavelength  $\lambda_g = \lambda_B$ , the reflectivity of the grating is given by  $R = \tanh^2(\kappa L)$ , where  $\kappa$  is the coupling coefficient and  $L$  is the grating length. For a uniform grating with small  $\kappa L$ , the reflectivity as a function of wavelength follows approximately a sinc<sup>2</sup> function.

We report here the first demonstration of efficient narrowband guided-wave Bragg filters in GaAs/GaAlAs rib waveguides with centre wavelengths at  $\sim 1.5 \mu\text{m}$ .

A schematic diagram of the rib grating filter is shown in Fig. 1. For this work, the Ga<sub>1-x</sub>Al<sub>x</sub>As buffer layer and the GaAs guiding layer were grown by MOCVD on an n<sup>+</sup>-GaAs

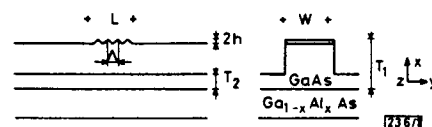


Fig. 1 Schematic diagram of a rib waveguide grating filter